

RESEARCH

Open Access



LINC01013 reverses bisphosphonate-impaired osteogenic differentiation of JBMMSCs by regulating intracellular translocation of ILF3

Jiaxin Song^{1,2}, Wanqing Wang², Xuanhe Feng¹, Haoqing Yang^{2*}, Zhaochen Shan^{1*} and Zhipeng Fan^{2,3,4*} 

Abstract

Background Bisphosphonate-related osteonecrosis of the jaw (BRONJ) is a serious complication associated with bisphosphonate (BP) therapy. Enhancement of the osteogenic differentiation of human jaw bone marrow mesenchymal stem cells (JBMMSCs) is a key issue in the treatment of BRONJ. In this study, we investigated the role and mechanism of LINC01013 in regulating osteogenic differentiation of JBMMSCs.

Methods Osteogenic differentiation of JBMMSCs was assessed in vitro using alkaline phosphatase (ALP), alizarin red staining (ARS), and western blotting. JBMMSCs transplanted into the backs of nude mice were used to detect JBMMSCs osteogenesis in vivo. Molecular mechanisms involved in JBMMSCs osteogenesis were evaluated using real-time fluorescence quantitative polymerase chain reaction, western blotting, fluorescence in situ hybridization, RNA pull-down, and RNA-seq.

Results Homeobox C8 (HOXC8) knockdown enhanced ALP activity, ARS, and expression of bone sialoprotein and osteocalcin in JBMMSCs under normal and BP stimulation conditions. HOXC8 negatively regulated LINC01013 expression. LINC01013 enhanced JBMMSCs osteogenic differentiation impaired by BP stimulation. Furthermore, LINC01013 regulated the expression of inflammation-related genes in JBMMSCs under BP conditions. LINC01013 formed a complex with ILF3. Two isoforms of ILF3 (NF90 and NF110) promoted the osteogenic differentiation of JBMMSCs under normal and BP conditions, depending on their nuclear localization. Additionally, NF90, which is located in the nucleus, inhibited the expression of NLR family pyrin domain containing 3 (NLRP3).

Conclusions In summary, HOXC8 negatively regulates LINC01013 to inhibit osteogenic differentiation of JBMMSCs under BP conditions. We also further clarified that LINC01013 binding to ILF3 affects ILF3 nuclear localization to

*Correspondence:

Haoqing Yang
yanghaoqing@mail.ccmu.edu.cn
Zhaochen Shan
shanzhch@mail.ccmu.edu.cn
Zhipeng Fan
zpfan@ccmu.edu.cn

Full list of author information is available at the end of the article



© The Author(s) 2025. **Open Access** This article is licensed under a Creative Commons Attribution-NonCommercial-NoDerivatives 4.0 International License, which permits any non-commercial use, sharing, distribution and reproduction in any medium or format, as long as you give appropriate credit to the original author(s) and the source, provide a link to the Creative Commons licence, and indicate if you modified the licensed material. You do not have permission under this licence to share adapted material derived from this article or parts of it. The images or other third party material in this article are included in the article's Creative Commons licence, unless indicated otherwise in a credit line to the material. If material is not included in the article's Creative Commons licence and your intended use is not permitted by statutory regulation or exceeds the permitted use, you will need to obtain permission directly from the copyright holder. To view a copy of this licence, visit <http://creativecommons.org/licenses/by-nc-nd/4.0/>.

regulate JBMMSCs osteogenic differentiation and regulates NLRP3/Caspase-1 pathway to affect JBMMSCs function under BP stimulation.

Keywords LINC01013, Human jaw bone marrow mesenchymal stem cells, Bisphosphonate-related osteonecrosis of the jaws, Osteogenesis, ILF3

Introduction

Bisphosphonates (BPs) are widely used in the treatment of bone-related conditions, however, BPs are associated with side effects. BP-related osteonecrosis of the jaw (BRONJ) is a serious complication of BP treatment that often occurs after dental procedures and is commonly associated with inflammatory dental diseases [1]. Currently, BRONJ is difficult to cure with no optimal treatment options except nonsurgical treatments such as local irrigation or surgical removal [2]. Several hypotheses, including the inhibition of bone remodeling, angiogenesis, and immunosuppression, underlying BRONJ pathogenesis have been proposed [1].

Early BP research focused on inhibiting osteoclast differentiation; however, recent studies suggest that BP affects bone marrow mesenchymal stem cells (BMSCs) function [3, 4]. BP has a concentration-dependent dual effect on BMSCs; lower concentrations of BP promote osteogenesis in BMSCs, and higher concentrations exert inhibitory effect [5–8]. Innovative strategies, including the introduction of vascular endothelial growth factor and geranylgeraniol, have been explored to counteract BP-induced impairments in cellular differentiation [9, 10]. However, the specific molecular mechanism by which BP inhibits jaw bone marrow mesenchymal stem cells (JBMMSCs) osteogenic differentiation remains unknown.

BRONJ exclusively affects the jaws and not the long bones [11]. The osteogenic differentiation potential of axial and jaw bone BMSCs differ, with jaw BMSCs having a higher osteogenic differentiation potential [11]. Axial and jaw bone BMSCs are also differentially sensitive to BP due to their different origins [12]. Identifying site-specific gene expression differences is pivotal for understanding the pathology of BRONJ. The HOX gene family is differentially regulated in jaw-derived and long-bone-derived BMSCs [13]. Homeobox C8 (HOXC8) inhibits the osteogenic differentiation of odontogenic stem cells [14]. Its expression in jaw-derived BMSCs is lower than that in long-bone-derived BMSCs [13]. However, the role of HOXC8 in JBMMSCs differentiation and function in BRONJ has not yet been investigated.

The human genome is extensively transcribed into RNA, with <2% of the transcriptome translated into proteins [15–17]. This highlights the prevalence of non-coding RNAs in the cellular landscape. Long non-coding RNAs (lncRNAs) are central players in cell biology and play essential regulatory roles in various processes

including cell differentiation and development [18]. Altered lincRNAs expression contributes to the development of bone metabolic diseases [19, 20]. In our previous study, we demonstrated that HOXC8 directly targets the LINC01013 promoter and regulates stem cell differentiation by modulating LINC01013 expression [21]. In addition, LINC01013 is involved in diverse regulatory roles in various biological processes and diseases: LINC01013 promotes cell invasiveness in anaplastic large-cell lymphoma [22], regulates cell stemness in liver cancer cells [23], improves DNA repair to alleviate endothelial cell dysfunction [24], and regulates the development of fibrosis in calcific aortic valve disease [25]. However, the role of LINC01013 as a direct downstream target of HOXC8 in the regulation of JBMMSCs function remains unclear.

With the development of proteomic and epigenetic technologies, the interactions between lncRNAs and RNA-binding proteins (RBPs) have gained considerable attention. Interleukin enhancer binding factor 3 (ILF3) is a double-stranded RNA-binding protein that has a 90 kDa isoform (NF90) and a 110 kDa isoform (NF110) [26]. ILF3 is implicated in a wide array of physiological functions, including viral infection response, mRNA transport, translation control, transcription, and cell cycle regulation [27]. Despite these insights, the complete spectrum of ILF3 involvement in osteogenesis, particularly in pathological conditions such as osteoporosis or BRONJ, remains poorly understood. Therefore, this study aimed to determine the role of ILF3 in BRONJ.

This study aims to bridge these gaps by exploring the roles of HOXC8 and LINC01013 in the osteogenic differentiation of JBMMSCs within a BP-stimulated environment. We sought to decipher the intricate regulatory relationship between these molecules under conditions mimicking BRONJ and, to understand how they influence JBMMSCs behavior and osteogenic potential in response to BP treatment. By focusing on this BRONJ-simulated scenario, this study elucidated the molecular dynamics of osteogenic differentiation under pathological conditions, offering insights into potential therapeutic targets and strategies to mitigate or reverse the detrimental effects of BP treatment on bone health.

Materials and methods

JBMMSCs culture

The experiments using human JBMMSCs were performed according to the ISSCR Guidelines for the Conduct of Human Embryonic Stem Cell Research. Alveolar

bone tissue was obtained from the Beijing Stomatological Hospital, Capital Medical University, and the study was approved by the Ethics Committee of the China Rehabilitation Research Center (CMUSH-IRB-KJ-PJ-2023-47). JBMMSCs were cultured in mesenchymal stem cell medium (ScienCell, Carlsbad, California) at 37 °C and 5% CO₂, as previously described [28]. JBMMSCs at passages 3–5 was used for subsequent experiments. JBMMSCs were treated with 5 μM zoledronic acid (Zol, Sigma). JBMMSCs were inoculated into osteogenic medium at a cell density of 2.0×10^5 cells/well as previously described [14].

Viral infection

The lentiviruses were obtained from GenePharma (Suzhou, China). The complementary DNA of human LINC01013, NF90, and NF110 was subcloned into an LV5 lentiviral vector. Overexpression vectors for NF90 and NF110 nuclear localization signal (NLS) deletion mutants (NF90/NF110ΔNLS) were constructed. Short hairpin RNA (shRNA) of HOXC8, LINC01013, and ILF3 were cloned into the LV2 lentiviral vector. After overnight incubation of JBMMSCs in 100 mm Petri dishes, the cells were exposed to lentivirus-containing medium for 12 h. The transfected cells were selected using puromycin (2 μg/mL) for 3 days. The shRNA target sequences are listed in Table S1.

Western blotting analysis

Protein was extracted and separated following previously published protocols [29]. The primary antibodies used were as follows: ILF3 (1:2,000, 19887-1-AP, Proteintech, Wuhan, China), ILF3 (1:2,000, A2496, Abclonal, Wuhan, China), HOXC8 (1:1,000, Wuhan, Proteintech), NLR family pyrin domain containing 3 (NLRP3, 1:1000, A5652, Abclonal, Wuhan, China), interleukin-1β (IL-1β, 1:1000, 12703 S, Cell Signaling Technology, Danvers, USA), Caspase-1 (1:1000, 22915-1-AP, Proteintech, Wuhan, China), osteocalcin (OCN; 1:1,000, A20800, Abclonal, Wuhan, China), bone sialoprotein (BSP; 1:1,000, bs-2668R, Bioss, Beijing, China), and GAPDH (1:5,000, Sigma-Aldrich, USA).

Real-time fluorescence quantitative polymerase chain reaction (RT-qPCR)

JBMMSCs were treated with TRIzol reagent (Invitrogen). Total mRNA was isolated using an Ultrapure RNA Kit (CW0581, CWBIO, Taizhou, China) and reverse-transcribed into cDNA, following the manufacturer's instructions. RT-qPCR was performed using the MagiSYBR Mixture PCR kit (CWBIO, Taizhou, China), following the manufacturer's instructions. The PCR primer sequences are listed in Table S2.

Alkaline phosphatase (ALP) and Alizarin red staining (ARS) analysis

Following five days of osteogenic induction, the collected cells were analyzed for ALP activity using an ALP activity kit (Sigma-Aldrich), following the manufacturer's instructions. JBMMSCs were fixed with 70% ethanol for 30 min and stained with 2% alizarin red (Sigma-Aldrich) two weeks after osteogenic induction.

RNA pull-down assays

RNA pull-down assays were performed as previously described [30]. Briefly, the collected JBMMSCs were extracted and transferred into centrifuge tubes. The cell lysates were mixed with in vitro-transcribed RNAs to form RNA-protein complexes. The complexes were purified using beads. Finally, bead-bound proteins were detected by western blotting after protein isolation from the beads.

Animal models

The nude mice (female, 8-week-old) were purchased from the Beijing Stomatological Hospital Animal Laboratory (Beijing, China). All animals were maintained on a normal light/dark cycle and were free to eat and drink. The nude mice were randomly divided into 7 groups with Vector group, LINC01013 group, Consh group, LINC01013sh group, Vector group, Vector+Zol group and LINC01013+Zol group, with 5 mice in each group. JBMMSCs were incubated with hydroxyapatite-tricalcium phosphate (HA/TCP) for 3 h at 37 °C as previously described [14]. The nude mice were intraperitoneally anesthetized using 1% pentobarbital sodium (40 mg/kg). Subsequently, the resulting mixture was transplanted subcutaneously into nude mice. Three months after transplantation, the nude mice were euthanized by cervical dislocation after isoflurane (RWD, China) inhalation. The transplanted tissue was removed for hematoxylin and eosin (HE), Masson's trichrome and immunofluorescence staining. All animal experiments followed the guidelines of the Animal Care and Use Committee of the Capital Medical University (approval number: KQYY-202309-006, Beijing, China). The work has been reported in line with the ARRIVE guidelines 2.0.

Histological and Immunofluorescence staining

The transplanted tissue was carefully removed after three months and fixed in 4% paraformaldehyde. Afterwards, the tissues were decalcified for four weeks in a solution containing 10% EDTA, followed by dehydration and paraffin embedding. Section (5 μm) were stained with hematoxylin and eosin (HE) and Masson's trichrome. For immunofluorescence staining, after dewaxing and rehydration, hydrated tissue sections were subjected to citrate antigen retrieval. Subsequently, the tissues were

blocked with goat serum at 37 °C for 30 min. The tissue was incubated with primary antibodies against OCN (1:200; bs-0470R, Bioss, Beijing, China), NLRP3 (1:200; A5652; Abclonal, Wuhan, China), ILF3 (1:200; 19887-1-AP; Proteintech, Wuhan, China), and Caspase-1 (1:200; 22915-1-AP; Proteintech, Wuhan, China) overnight. The secondary antibody used was Alexa Fluor 594 goat anti-rabbit IgG (1:500, Life Technologies, USA). The nuclei were stained with DAPI.

RNA-seq and bioinformatic analysis

Total RNA was isolated from JBMMSCs-LINC01013sh and JBMMSCs-Consh. RNA-seq and bioinformatics analyses were performed at SHANGHAI BIOTREE BIOTECH Co., LTD (Shanghai, China). The negative logarithm of the p value (-LgP) was calculated to represent the correlation between gene expression and Gene Ontology (GO) functions or pathways.

Fluorescence in situ hybridization (FISH)

The FISH probe of LINC01013 was obtained from GenePharma. The FISH assay was performed according to the guidelines provided in the FISH Kit Manual (GenePharma). Briefly, cells were fixed in 4%

paraformaldehyde and hybridized with probe mixture solution (4 μM). Nuclei were stained with DAPI.

Statistical analyses

Statistics were calculated using GraphPad Prism 9.0 software.

Comparisons between groups were performed using Student’s *t*-test or one-way analysis of variance. Results are presented as mean ± standard deviation, and *p*-values less than 0.05 were considered statistically significant.

Results

HOXC8 Inhibition promoted JBMMSCs osteogenic differentiation under normal and Zol-stimulated conditions

To evaluate the effects of HOXC8 on osteogenesis, HOXC8 shRNA lentivirus was used to inhibit HOXC8 expression in JBMMSCs. Western blotting confirmed HOXC8 knockdown in JBMMSCs (Fig. 1A). Correspondingly, HOXC8 downregulation enhanced ALP activity, indicating increased osteoblastic function in JBMMSCs (Fig. 1B). This was further validated by ARS analysis, which demonstrated that HOXC8 knockdown significantly enhanced JBMMSCs mineralization (Fig. 1C). Additionally, western blotting analysis revealed an

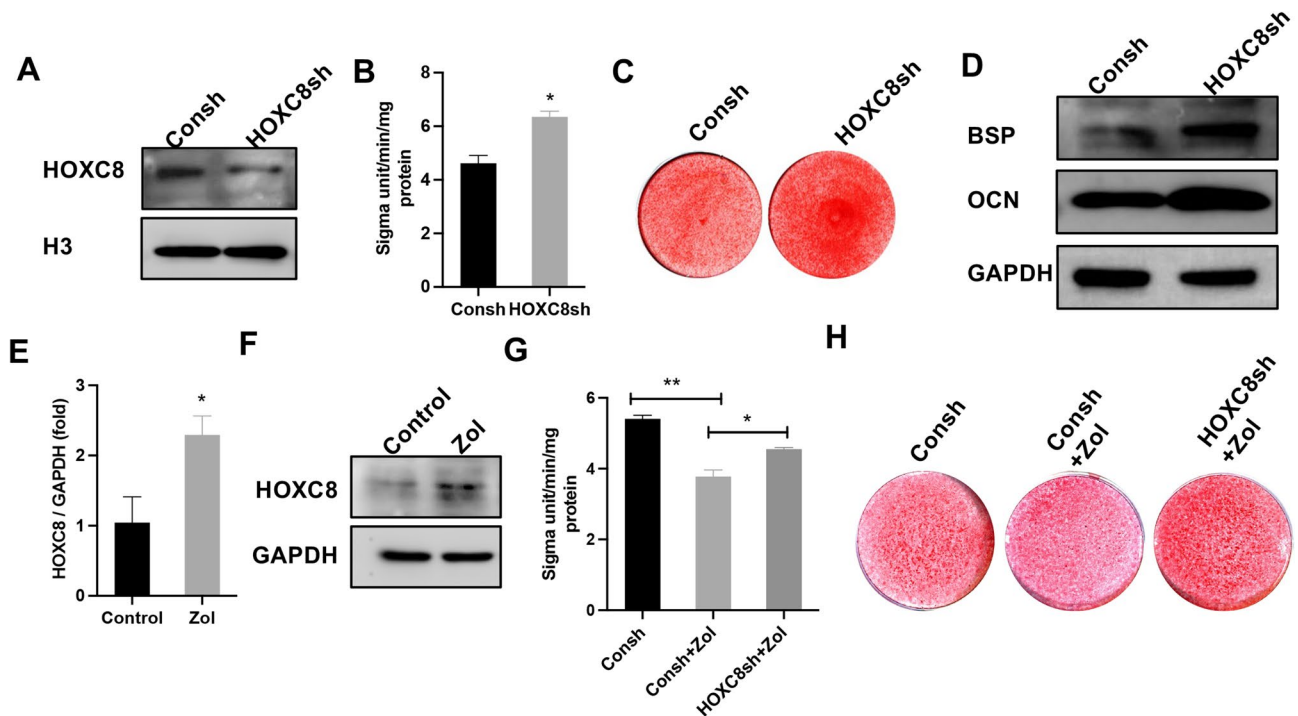


Fig. 1 HOXC8 inhibited Zol-stimulated JBMMSCs osteoblastic function. (A) HOXC8 protein expression level in JBMMSCs. (B) HOXC8 knockdown enhanced ALP activity in JBMMSCs. (C) ARS demonstrating that HOXC8 knockdown elevated mineralization in JBMMSCs. (D) Western blotting analysis of BSP and OCN expression. (E) RT-qPCR and (F) western blotting showing increased HOXC8 expression following Zol-treatment. (G) HOXC8 knockdown promoted ALP activity in JBMMSCs during Zol-treatment. (H) ARS demonstrating that HOXC8 knockdown enhanced mineralization in Zol-treated JBMMSCs. Data are represented as mean ± standard deviation (*n* = 3), and **P* < 0.05, ***P* < 0.01 (Student’s *t*-test or one-way analysis of variance). Full-length blots/gels are presented in Figure S1

increased expression of BSP and OCN upon HOXC8 knockdown, indicative of osteoblastic marker upregulation (Fig. 1D). RT-qPCR and western blotting analysis confirmed HOXC8 upregulation in JBMMSCs treated with Zol (Fig. 1E, F). Under Zol treatment, ALP activity and ARS increased osteogenic activity and mineralization in JBMMSCs with HOXC8 knockdown (Fig. 1G, H). These results indicate that HOXC8 suppression under Zol stimulation significantly promotes JBMMSCs osteogenic differentiation.

LINC01013 enhanced JBMMSCs osteogenic differentiation

Our previous results suggest that LINC01013 is a downstream target gene of HOXC8 [21]. RT-qPCR revealed a significant increase in LINC01013 mRNA levels in HOXC8 silenced JBMMSCs, suggesting that HOXC8 negatively regulates LINC01013 expression (Fig. 2A). A time-dependent study showed a consistent increase in LINC01013 expression over 7 days after osteogenic induction (Fig. 2B), suggests that LINC01013 may regulate JBMMSCs osteogenic differentiation. Therefore, we verified the effects of LINC01013 on the osteogenic differentiation potential of JBMMSCs. The overexpression of LINC01013 was confirmed by RT-qPCR (Fig. 2C). LINC01013 knockdown was confirmed using RT-qPCR (Fig. 2D). LINC01013 overexpression markedly increased ALP activity and mineralization in JBMMSCs (Fig. 2E, G). Furthermore, ALP and ARS activities indicated a significant decrease in osteogenic activity and mineralization in JBMMSCs with LINC01013 knockdown (Fig. 2E, H). We also detected the expression of BSP and OCN in LINC01013 overexpressed and knockdown JBMMSCs. Western blotting analysis showed a significant increase in BSP and OCN expression in JBMMSCs overexpressing LINC01013, indicating enhanced osteogenic differentiation one week after induction (Fig. 2I). A reduction was observed in BSP and OCN expression in JBMMSCs with LINC01013 knockdown (Fig. 2J).

Next, we determined whether LINC01013 affects the osteogenesis of JBMMSCs *in vivo*. HE (Fig. 2K, N, P) and Masson staining (Fig. 2L) revealed that bone mineralized tissue regeneration in the JBMMSCs-LINC01013 transplanted tissues was greater than that in the control group. In addition, the degree of bone mineralized tissue regeneration in the JBMMSCs-LINC01013sh group was lower than that in the control group. These findings suggest that bone formation is reduced in the absence of LINC01013. Moreover, immunofluorescent staining (Fig. 2M, O, and Q) showed that LINC01013 overexpression enhanced OCN expression, whereas LINC01013 knockdown reduced OCN expression. These results suggest that LINC01013 plays an essential role in osteogenic differentiation promotion and bone formation in JBMMSCs.

Restorative effects of LINC01013 overexpression on Zol-treated JBMMSCs

To investigate whether LINC01013 could rescue the impaired function in Zol-treated JBMMSCs, LINC01013-overexpressing JBMMSCs were exposed to Zol. Zol treatment decreased the LINC01013 mRNA levels (Fig. 3A). We then evaluated the effect of LINC01013 on the osteogenic differentiation potential of Zol-induced JBMMSCs. ALP activity and ARS analyses revealed that LINC01013 overexpression partially restored the osteogenic potential that was reduced by Zol stimulation (Fig. 3B, C), confirming the role of LINC01013 in osteogenic differentiation under Zol treatment.

Furthermore, HE and Masson staining provided a clear view of the restored tissue architecture in JBMMSCs overexpressing LINC01013 under Zol treatment (Fig. 3D-G). The cells displayed a more organized, denser, and structured extracellular matrix compared to the Zol-treated controls. Additionally, immunofluorescence staining revealed increased OCN expression in JBMMSCs overexpressing LINC01013, even after Zol stimulation (Fig. 3H, I). These results indicated that LINC01013 may counteract the adverse effects of Zol on JBMMSCs and support the restoration of osteogenic potential in bone tissue.

Identification of differentially expressed mRNAs in JBMMSCs-LINC01013sh and bioinformatic analysis of RNA-seq data

To further investigate the mechanism by which LINC01013 regulates the osteogenic differentiation of JBMMSCs, RNA-seq and bioinformatic analyses were performed on LINC01013 knockdown JBMMSCs. RNA-seq results showed that 1,438 mRNAs were differentially expressed ($|\log_2FC| > 1$, $FDR < 0.05$) in the JBMMSCs-LINC01013sh and consh groups; 1,124 mRNAs were upregulated and 314 were downregulated (Table S3). Five differentially expressed genes, including mesenteric estrogen dependent adipogenesis (MEDAG), vitrin (VIT), matrix Gla protein (MGP), gasdermin C (GSDMC), and iodothyronine deiodinase 2 (DIO2), were selected from the sequencing results to validate the accuracy and credibility of the RNA-seq results. RT-qPCR results (Fig. 4A, B) showed MEDAG, VIT, MGP, GSDMC, and DIO2 upregulation in the JBMMSCs-LINC01013sh group. Conversely, the overexpression group exhibited MEDAG, VIT, MGP, GSDMC, and DIO2 downregulation. These results are consistent with those of RNA-seq. To further clarify the potential functions of the differentially expressed genes, GO enrichment and KEGG pathway analyses were performed. The top 20 signaling pathways enriched in the set of genes included the calcium and PI3K-AKT signaling pathways (Fig. 4C). GO functional analysis revealed that the differentially expressed genes

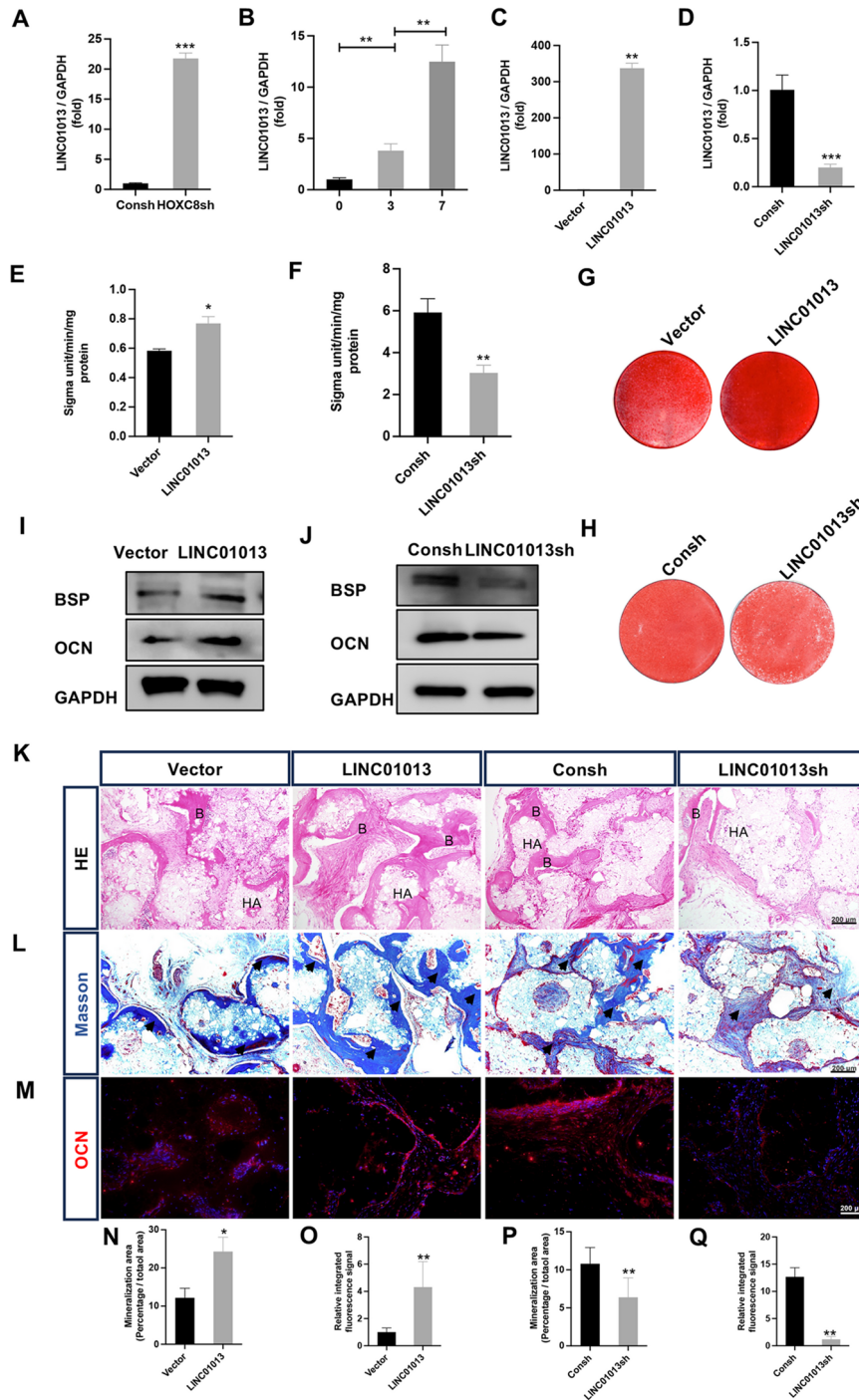


Fig. 2 LINC01013 enhanced JBMMSCs osteogenic differentiation. **(A)** RT-qPCR demonstrating the enhancement of LINC01013 in HOXC8-silenced JBMMSCs compared to controls. **(B)** A time-dependent study revealed a consistent augmentation in LINC01013 expression over a 7-day period under osteogenic inducing conditions. **(C)** LINC01013 overexpression efficiency validated with RT-qPCR. **(D)** RT-qPCR confirming LINC01013 knockdown. **(E)** ALP activity assays and **(G)** ARS exhibit a notable increase in mineralization of LINC01013 overexpressing JBMMSCs. **(F)** ALP activity assays and **(H)** ARS results demonstrated a notable decrease in mineralization in LINC01013 knockdown JBMMSCs. **(I, J)** Western blotting analysis of BSP and OCN expression. **(K)** HE and **(L)** Masson staining. B points to the formation of bone-like tissue. HA points to hydroxyapatite. Arrows represent newly formed bone-like tissue. **(M)** Immunofluorescence staining for OCN (red) indicates enhanced osteogenic activity in LINC01013-overexpressing JBMMSCs, with weaker signals in LINC01013-knockdown groups. **(N, P)** Quantitative analysis of mineralized areas and **(O, Q)** OCN expression levels in vivo. Data are represented as mean \pm standard deviation ($n=3$), and $*P < 0.05$, $**P < 0.01$, $***P < 0.001$ (Student's t-test or one-way analysis of variance). Full-length blots/gels are presented in Figure S2

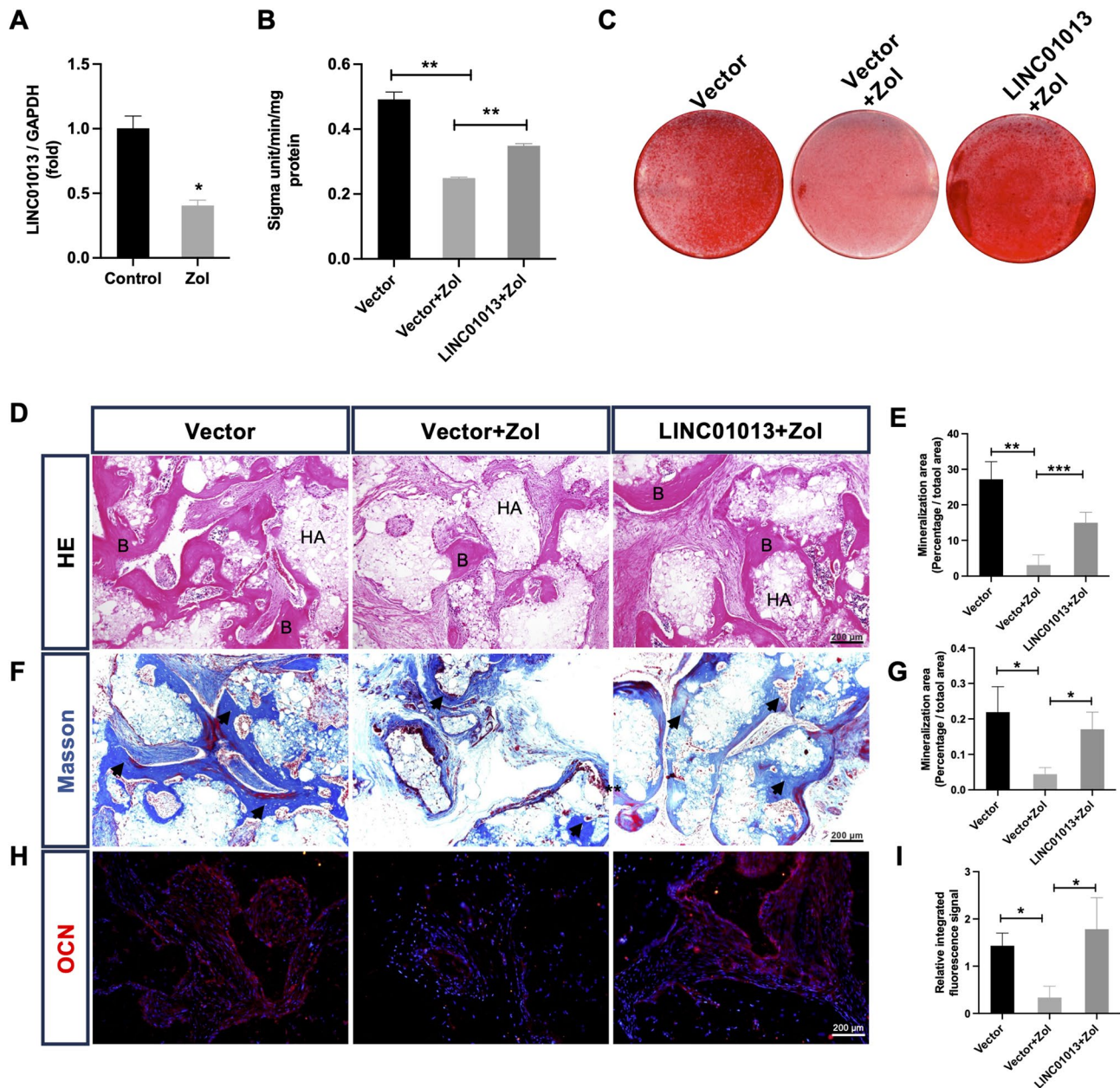


Fig. 3 LINC01013 rescued osteogenic differentiation of Zol-stimulated JBMSCs. **(A)** RT-qPCR analysis showing Zol decreased LINC01013 expression in JBMSCs. **(B)** ALP activity assays showing that overexpression of LINC01013 partially restored ALP activity in Zol-stimulated cells. **(C)** ARS staining illustrating reduced mineralized nodule formation in JBMSCs treated with Zol, with partial recovery observed in the LINC01013-overexpression group. **(D)** H&E and **(F)** Masson staining demonstrating that LINC01013 overexpression under Zol stimulation could restore the osteogenic ability of JBMSCs. B points to the formation of bone-like tissue. HA points to hydroxyapatite. Arrows represent newly formed bone-like tissue. **(H)** Immunofluorescence staining of OCN (red) showing significantly reduced osteogenic activity in Zol-treated JBMSCs, with increased signals in the LINC01013 + Zol group. **(E, G)** Quantitative analysis of mineralized areas and **(I)** OCN expression levels in vivo. Data are represented as mean \pm standard deviation ($n=3$), and * $P < 0.05$, ** $P < 0.01$, *** $P < 0.001$ (Student's t-test or one-way analysis of variance)

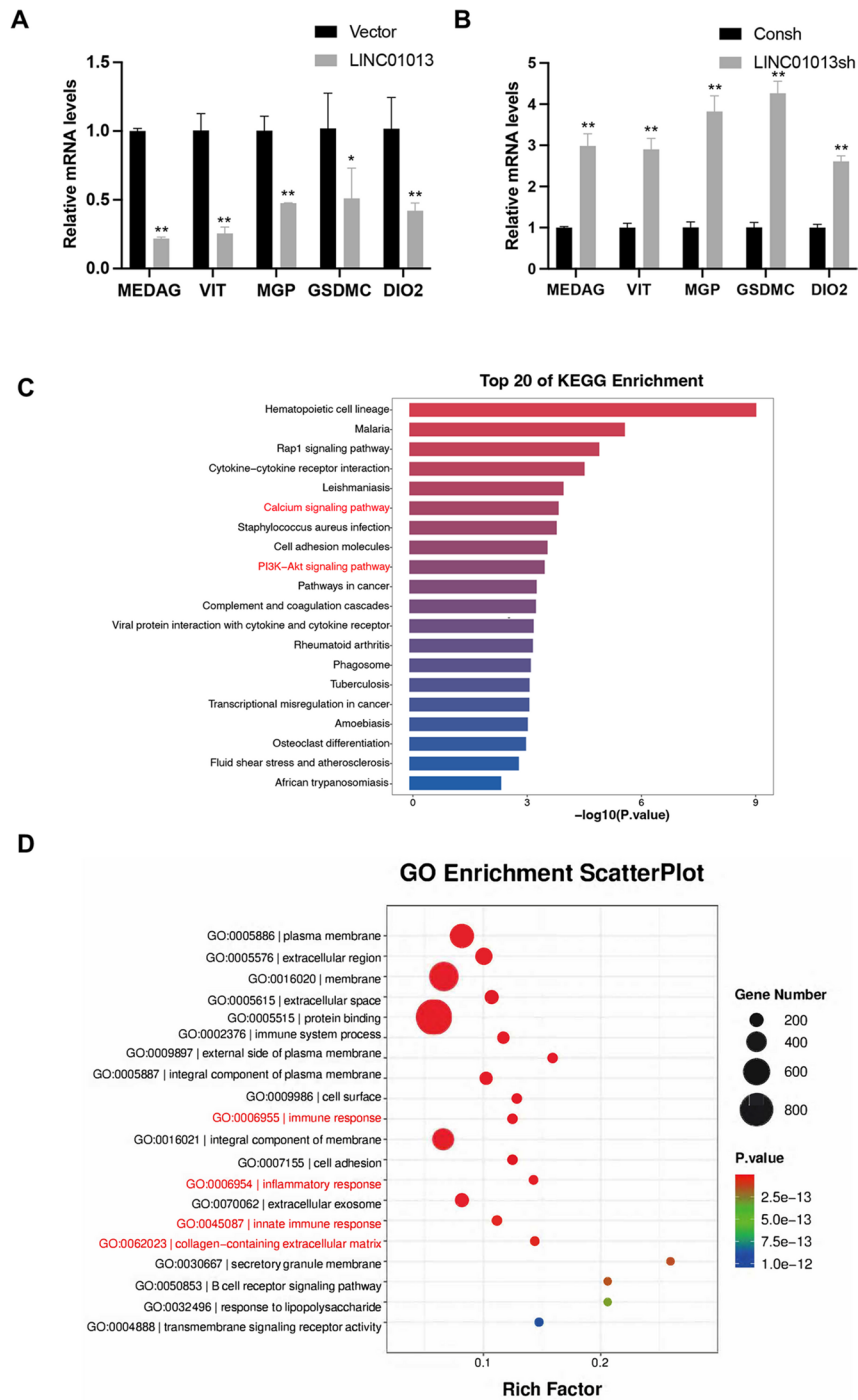


Fig. 4 RNA-seq data analysis of LINC01013 knockdown JBMSCs. **(A)** RT-qPCR analysis showing significantly decreased mRNA levels of MEDAG, VIT, MGP, GSDMC, and DIO2 in LINC01013-overexpressing JBMSCs compared to the vector control. **(B)** Increased expression of mRNA levels of MEDAG, VIT, MGP, GSDMC and DIO2 in LINC01013 knockdown JBMSCs. **(C)** KEGG pathway enrichment analysis of differentially expressed genes highlights pathways significantly affected by LINC01013 knockdown. **(D)** GO enrichment analysis visualizing biological processes influenced by LINC01013. Data are represented as mean \pm standard deviation ($n = 3$), and $*P < 0.05$, $**P < 0.01$ (Student's t-test)

correlated with binding proteins, inflammatory response, immune response, and I collagen-containing extracellular matrix (Fig. 4D).

LINC01013 overexpression inhibited inflammation-related genes expression in JBMMSCs

Further bioinformatic analysis of the differentially expressed genes focused on understanding the specific inflammatory pathways influenced by LINC01013. To investigate the anti-inflammatory mechanism of LINC01013, we used RT-qPCR and western blotting to

quantify transcriptional and translational changes in key inflammasome components (Caspase-1, NLRP3, and IL-1 β). The RT-qPCR and western blotting results showed that LINC01013 overexpression led to a decrease in inflammation-related genes including Caspase-1, NLRP3, and IL-1 β , suggesting that LINC01013 potentially exerts anti-inflammatory effects (Fig. 5A-D). LINC01013 overexpression in Zol-treated JBMMSCs resulted in decreased levels of these markers, further indicating the suppressive effect of LINC01013 on inflammasome-related genes.

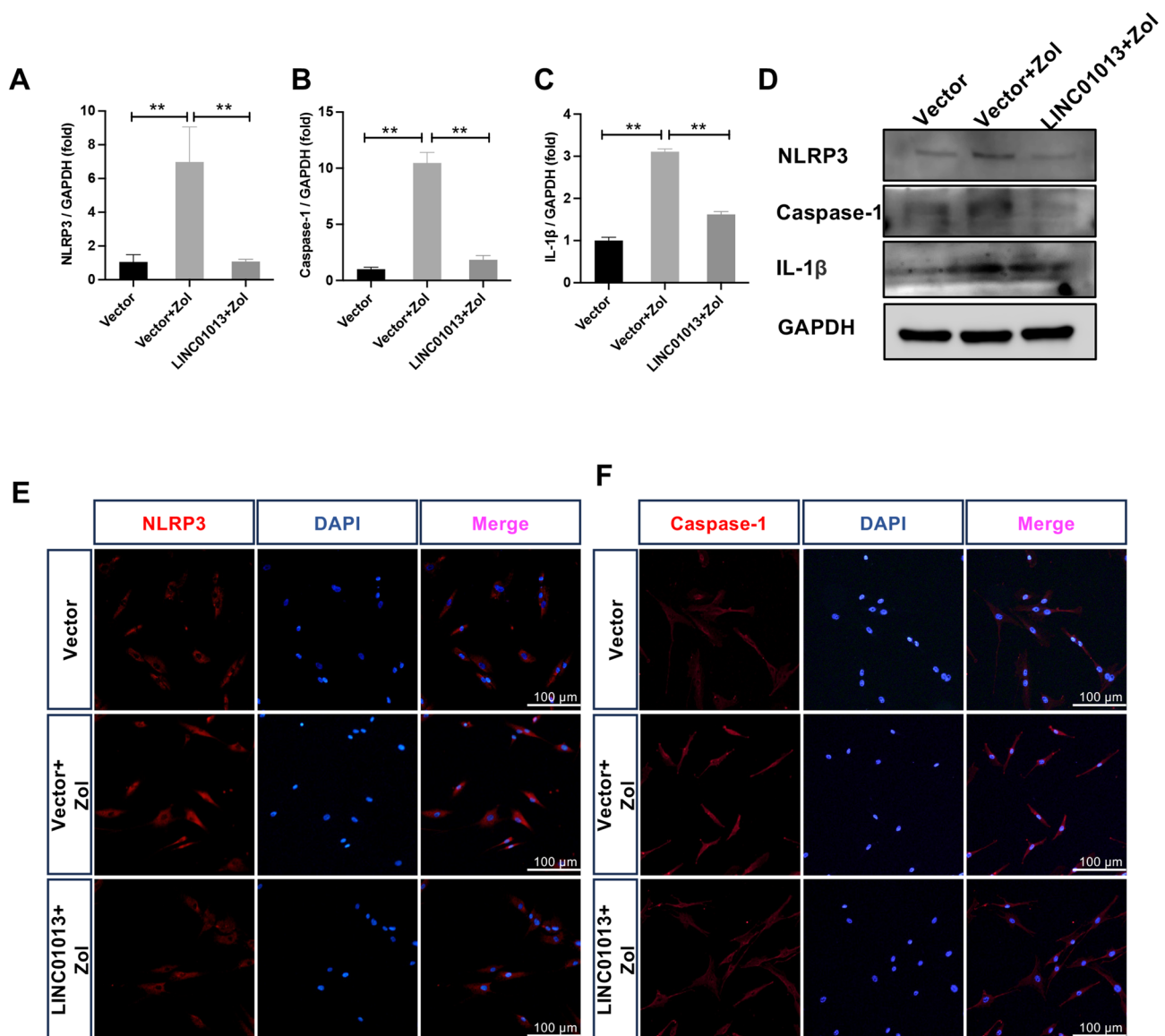


Fig. 5 LINC01013 regulated inflammation-related genes expression in Zol-treated JBMMSCs. (A-C) RT-qPCR analysis showing significantly increased mRNA levels of NLRP3 (A), Caspase-1 (B), and IL-1 β (C) in Zol-treated JBMMSCs, while these mRNA levels decreased in LINC01013 overexpressing JBMMSCs. (D) Western blotting analysis demonstrating elevated protein levels of NLRP3, Caspase-1, and IL-1 β in Zol-treated JBMMSCs, which were reversed in the LINC01013 expression group. Immunofluorescence staining of NLRP3 (red) (E) and Caspase-1 (red) (F) in JBMMSCs overexpressing LINC01013 and the control JBMMSCs under Zol treatment. Nuclei (DAPI) are in blue. Data are represented as mean \pm standard deviation ($n = 3$), and $^{**}P < 0.01$ (one-way analysis of variance). Full-length blots/gels are presented in Figure S3

Immunofluorescence staining was performed to visualize NLRP3 and Caspase-1 in JBMMSCs after Zol treatment. Following Zol treatment, NLRP3 and Caspase-1 levels increased, indicative of inflammasome activation. Notably, JBMMSCs overexpressing LINC01013 subjected to Zol exposure exhibited a marked reduction in NLRP3 and Caspase-1 levels, indicating the negative regulatory influence of LINC01013 on the inflammasome machinery (Fig. 5E, F).

LINC01013 formed an RNA-protein complex with ILF3

The functions of lncRNAs are closely associated with their subcellular localization [31]. Thus, we employed RNA-FISH to detect the subcellular localization of LINC01013 in JBMMSCs. The results revealed the predominant nuclear presence of LINC01013 in JBMMSCs (Fig. 6A). After identifying the subcellular localization of LINC01013, predicting the proteins interacting with it was essential for gaining a deeper understanding of its molecular mechanisms. Through bioinformatics prediction of potential LINC01013-binding proteins, the results indicated that LINC01013 may form a protein complex with ILF3 (Fig. 6B). To validate this prediction, we used RNA pull-down assay. The results demonstrated the interaction between LINC01013 and ILF3 (Fig. 6C).

NF90 and NF110 are primarily DNA- and RNA-binding proteins that play significant roles in the regulation of various RNA metabolism processes [27]. Notably, Zol stimulation did not influence the transcription and translation of NF90 or NF110, as demonstrated by RT-qPCR and western blotting (Fig. 6D, E).

NF90 and NF110 promoted JBMMSCs osteogenic differentiation

To detect the effect of NF90 and NF110 on osteogenic differentiation in JBMMSCs, ILF3 was silenced using lentiviral ILF3 shRNA in JBMMSCs, and the knockdown efficiency was verified by western blotting (Fig. 7A). The corresponding ALP and ARS activities indicated a significant decrease in osteogenic activity and mineralization in ILF3 knockdown JBMMSCs (Fig. B, C). Western blotting revealed reduced BSP and OCN expression in ILF3 knockdown JBMMSCs one week after induction (Fig. 7D). To test the effect of NF90 and NF110 on the osteogenic differentiation of JBMMSCs, we constructed NF90- and NF110-overexpressing JBMMSCs, respectively. The efficiency of NF90 and NF110 overexpression was validated using western blotting (Fig. 7E). The cells were then cultured in osteogenic induction medium. NF90 and NF110 overexpression markedly increased

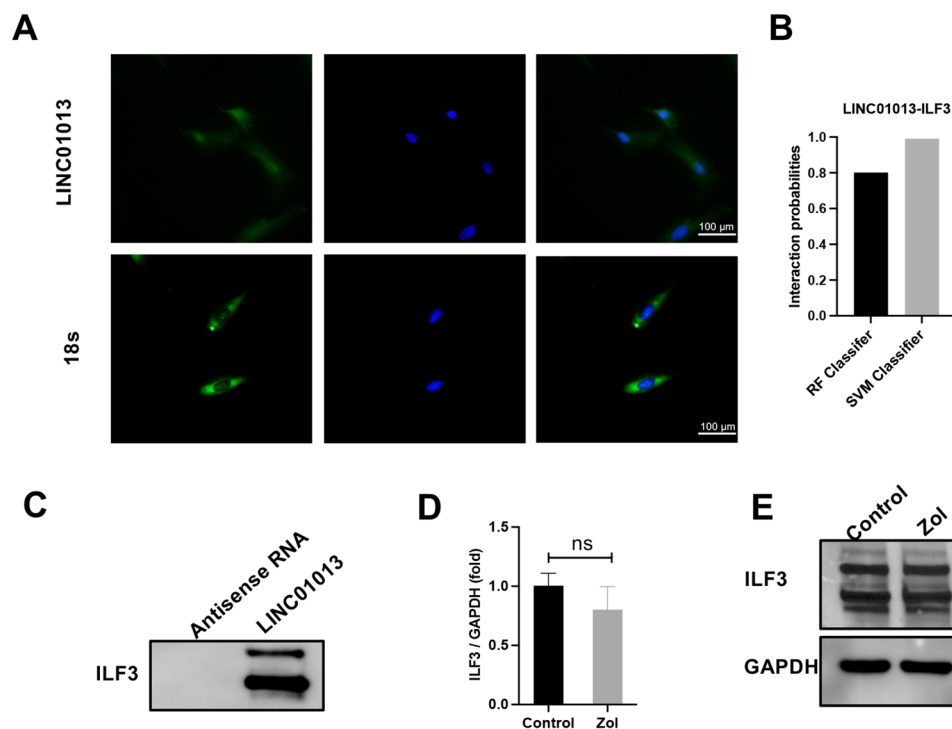


Fig. 6 LINC01013 formed a complex with ILF3. **(A)** RNA FISH was utilized to determine LINC01013 RNA molecules within the cells. The localization of 18s ribosomal RNA is shown as a positive control for the FISH technique. Nuclei (DAPI) are in blue. **(B)** Predictive analyses showing an interaction between LINC01013 and ILF3. **(C)** Western blotting validated the presence of ILF3 protein in cell lysates treated with an antisense probe against LINC01013, confirming the interaction at the protein level. RT-qPCR **(D)** and western blotting **(E)** revealed that Zol treatment did not change the levels of ILF3 in JBMMSCs after Zol treatment. Data are represented as mean \pm standard deviation ($n=3$), and ns, not significant (Student's t-test). Full-length blots/gels are presented in Figure S4

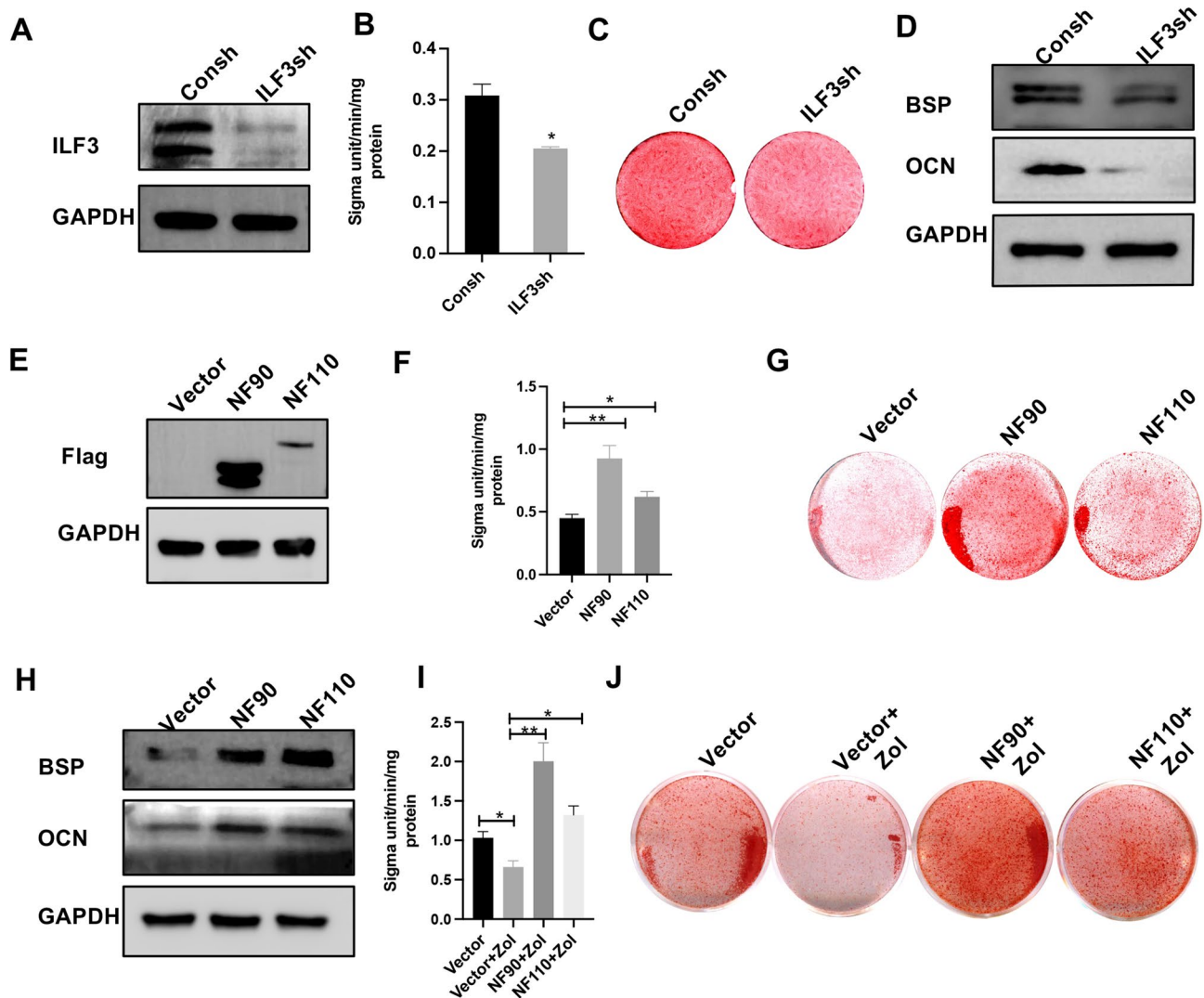


Fig. 7 NF90 and NF110 enhanced osteogenic differentiation of JBMMSCs under normal and Zol conditions. **(A)** Western blotting confirming the ILF3 knockdown in JBMMSCs. **(B)** ILF3 knockdown decreased ALP activity in JBMMSCs. **(C)** ARS results showed that ILF3 knockdown repressed the mineralization capacity of JBMMSCs. **(D)** Western blotting revealing a reduction in the levels of BSP and OCN in ILF3 knockdown JBMMSCs. **(E)** Western blotting confirming the overexpression efficiency of ILF3 variants NF90 and NF110. **(F)** ALP activity assay showing increased ALP activity in JBMMSCs overexpressing NF90 and NF110. **(G)** ARS results indicating enhanced mineralization in NF90 and NF110 overexpressing JBMMSCs. **(H)** Western blotting results showing an increase in the levels of BSP and OCN in NF90 and NF110 overexpression JBMMSCs. ALP **(I)** and ARS **(J)** results showed that NF90 and NF110 overexpression increased the mineralization of JBMMSCs under Zol stimulation. Data are presented as mean \pm standard deviation ($n=3$), and $*P < 0.05$, $**P < 0.01$ (Student's t-test or one-way analysis of variance). Full-length blots/gels are presented in Figure S5

ALP activity and mineralization in JBMMSCs, indicating their positive roles in osteogenic differentiation (Fig. 7E, G). Western blotting showed increased BSP and OCN expression in JBMMSCs overexpressing NF90 and NF110, indicating enhanced osteogenic differentiation one week after induction (Fig. 7H). Then, we evaluated the potential of NF90 and NF110 in rescuing the osteogenic differentiation of Zol-stimulated JBMMSCs. ALP and ARS activity revealed that NF90 and NF110 overexpression partially restored the osteogenic potential that was reduced by Zol stimulation (Fig. 7I, J).

Zol inhibited osteogenesis via NF90 and NF110 nuclear translocation alteration

ILF3 function correlates with its intracellular localization [32, 33]. Under basal conditions, ILF3 was predominantly localized within the nucleus, as evidenced by immunofluorescence staining. After Zol exposure, ILF3 translocated from the nucleus to the cytoplasm, suggesting that Zol treatment alters intracellular distribution of ILF3 (Fig. 8A). Furthermore, we determined the effect of LINC01013 on the nuclear-to-cytoplasmic ratio of ILF3. JBMMSCs overexpressing LINC01013 exhibited different responses to Zol treatment. The persistence of ILF3

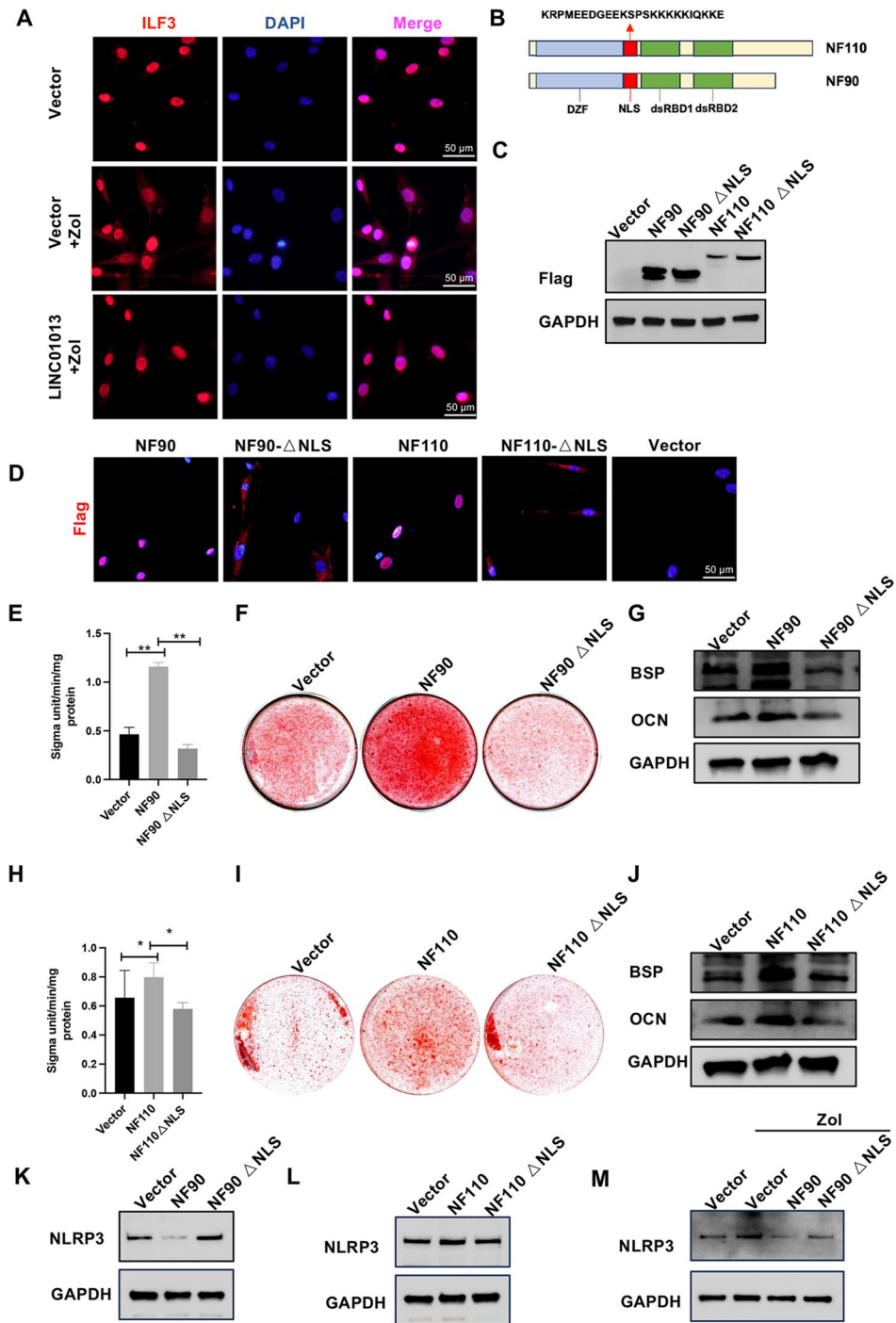


Fig. 8 NF90 and NF110 regulated JBMMSCs osteogenic differentiation through intracellular localization. **(A)** Immunofluorescence analysis showing the localization of ILF3 in JBMMSCs under control, Zol treatment, and LINC01013 overexpression conditions. Nuclei were stained with DAPI (blue). **(B)** A schematic representing the NLS within the ILF3 protein and its variants, NF90 and NF110. **(C)** Western blotting showing the expression of Flag-tagged ILF3 and their NLS-deleted mutants (NF90ΔNLS, NF110ΔNLS) in JBMMSCs. **(D)** Immunofluorescence staining for Flag (red) showing nuclear localization of NF90 and NF110, while the NLS-deleted mutants exhibited reduced nuclear retention. **(E-G)** The ALP activity assay **(E)**, ARS **(F)**, and Western blotting **(G)** showed that NF90 overexpressing JBMMSCs had a significantly higher osteogenic differentiation capacity compared to controls, whereas NF90ΔNLS overexpressing JBMMSCs had a reduced osteogenic differentiation capacity compared to NF90 overexpressing JBMMSCs. **(H-J)** ALP activity **(H)**, ARS staining **(I)**, and western blotting **(J)** demonstrated enhanced osteogenic differentiation in NF110 overexpressing JBMMSCs compared to controls, while NF110ΔNLS reduced differentiation relative to NF110. **(K)** Western blot analysis of NLRP3 expression levels in NF90 and NF90ΔNLS overexpressing JBMMSCs. **(L)** The protein level of NLRP3 in NF110 and NF110ΔNLS overexpressing JBMMSCs. **(M)** Western blot analysis showing the levels of NLRP3 in NF90 and NF90ΔNLS overexpressing JBMMSCs under Zol treatment. Data are presented as mean ± standard deviation ($n = 3$), and $*P < 0.05$, $***P < 0.01$ (one-way analysis of variance). Full-length blots/gels are presented in Figure S6-7

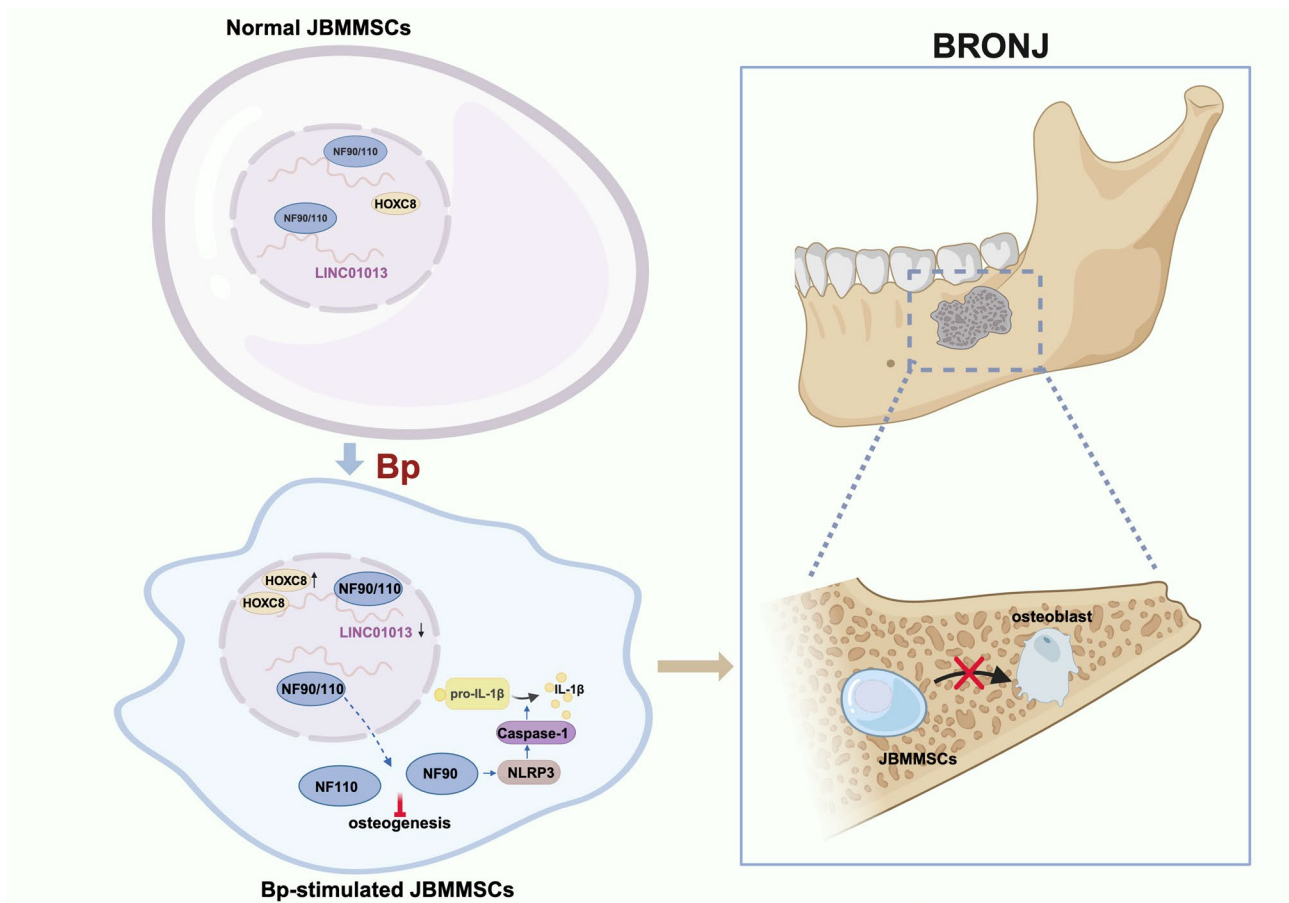


Fig. 9 Mechanism diagram of LINC01013 reversing bisphosphonate-impaired osteogenic differentiation of JBMMSCs by regulating intracellular translocation of ILF3

within the nuclei of these cells implied that LINC01013 overexpression could modulate the intracellular trafficking of ILF3 (Fig. 8A).

To determine whether the NLS sequences are critical for the function of NF90 and NF110 in promoting osteogenesis, a mutant of NF90 and NF110 lacking the NLS sequences (NF90/NF110ΔNLS) was used [33] (Fig. 8B). Western blotting confirmed the overexpression efficacy of NF90, NF110, and NF90/NF110ΔNLS (Fig. 8C). To assess the subcellular localization of the NF90/NF110ΔNLS mutant, immunofluorescence staining was performed, which confirmed its cytoplasmic localization (Fig. 8D). Then, we assessed the osteogenic differentiation of JBMMSCs overexpressing NF90, NF110 and NF90/NF110ΔNLS. ALP activity assay, ARS, and western blotting results showed that NF90/NF110ΔNLS overexpression attenuated the potential of NF90/NF110 to promote JBMMSCs osteogenic differentiation (Fig. 8E-J).

We also investigated the potential regulatory role of ILF3 in NLRP3 expression in JBMMSCs. Western blotting showed that only NF90, which is located in the nucleus of the cell, has a negative regulatory role in

NLRP3 under normal conditions and Zol stimulation (Fig. 8K-M). These findings suggest that LINC01013 regulates the nuclear translocation of ILF3 and influences the osteogenic differentiation of JBMMSCs, with NF90 playing a critical role in modulating NLRP3 expression after Zol treatment.

Taken together, the mechanism by which LINC01013 regulated the osteogenic differentiation of JBMMSCs was shown in Fig. 9. HOXC8 negatively regulates LINC01013 to inhibit osteogenic differentiation of JBMMSCs under BP condition. LINC01013 binding to ILF3 affects the nuclear localization of ILF3 and regulates the NLRP3/Caspase-1 pathway to affect the function of JBMMSCs under BP stimulation (Fig. 9).

Discussion

In this study, we investigated the role and mechanism of HOXC8/LINC01013 during the osteogenic differentiation of JBMMSCs under Zol stimulation. We comprehensively elucidated the complex mechanisms underlying the mechanisms in which Zol inhibits osteogenic differentiation of JBMMSCs. We demonstrated that in response

to Zol treatment, HOXC8 exerts an inhibitory role and LINC01013 exerts an enhanced role in osteogenic differentiation. Furthermore, we highlight that ILF3 plays a pivotal role in this differentiation process, revealing its potential as a therapeutic target.

We demonstrated that HOXC8 negatively regulates the osteogenic differentiation of JBMMSCs. ALP activity represents the early stages of JBMMSCs osteogenic differentiation [34]. HOXC8 knockdown increases ALP activity in JBMMSCs. BSP and OCN play critical roles in mineralization and are major non-collagenous proteins in the extracellular matrix of the bone [35, 36]. Consistently, HOXC8 knockdown enhanced BSP and OCN expression in JBMMSCs. To confirm our observations, we analyzed calcium deposition, an indicator of the late stages of BMSCs osteogenic differentiation [37], and found that HOXC8 is involved in the Zol-induced negative regulation of JBMMSCs osteogenic differentiation.

Numerous lncRNAs are essential for the pathogenesis of bone diseases. We have previously shown that HOXC8 binds to the LINC01013 promoter to suppress LINC01013 expression [14]. In contrast to HOXC8, LINC01013 expression was decreased in Zol-stimulated JBMMSCs. Both in vitro and in vivo results demonstrated that LINC01013 rescued the Zol-induced impaired osteogenic differentiation of JBMMSCs. These findings indicate that HOXC8/LINC01013 plays an essential role in Zol-induced osteogenic differentiation impairment in JBMMSCs.

We confirmed that LINC01013 was located in the nucleus of JBMMSCs. The interaction between lncRNAs and proteins is an important mechanism through which lncRNAs exert their regulatory functions [38]. We demonstrated an interaction between LINC01013 and ILF3. Previous studies have shown that the lncRNA PLXDC2-OT binds to the SIRT7/RBM6 protein complex to impair its binding and deacetylation function in the OSX promoter, thereby enhancing the osteogenic differentiation of MSCs [39]. It has also been shown that the lincRNA myocardial infarction-associated transcript (MIAT) is a regulator of the early stages of Th17 cell differentiation. Mechanistic studies have shown that signal transducer and activator of transcription 3 (STAT3) induces MIAT expression by binding to the MIAT promoter [40]. Therefore, the RNA-protein complex is central to the regulation of stem cell differentiation.

ILF3 shuttles between the nucleus and cytoplasm, and is composed of a bipartite nuclear localization domain, an RNA-binding domain with two dsRBMs, and an arginine- and glycine-rich C-terminal domain [26]. NF90/NF110 proteins are primarily involved in regulating gene expression by shuttling between the nucleus and cytoplasm [41]. Previous studies have shown that the regulatory roles of NF90 and NF110 in modulating bone

marrow maturation and IFN responses depend on their nuclear localization [33]. Furthermore, ILF3 is involved in hyperlipidemia-induced atherosclerotic calcification. The molecular mechanism involves ILF3 promotion of calcification in human aortic vascular smooth muscle cells by acting on the promoter region that regulates bone morphogenetic protein 2 (BMP2) and signal transducer and activator of transcription 1 (STAT1), thereby regulating the transcription of BMP2 and STAT1 [42]. Accordingly, the function of ILF3 is closely associated with its nuclear localization. Consequently, we investigated the effect of Zol on the intracellular localization of ILF3 in JBMMSCs. We found that LINC01013 regulates ILF3 translocation between the nucleus and cytoplasm under Zol stimulation. Previous studies have demonstrated that phosphorylation of ILF3 leads to its translocation from the nucleus to the cytoplasm [43]. There are also studies confirming that lncRNA-BTX prevents ILF3's migration to the cytoplasm from the nucleus by enhancing the interaction between ILF3 and ILF2 [32]. However, the molecular mechanism by which LINC01013 regulates ILF3 localization requires further study. Moreover, our results showed that NF90 and NF110 osteogenic differentiation promotion of JBMMSCs depended on their nuclear localization. NF90 interacts with the 3'-UTR region of various mRNAs such as poly (ADP-ribose) polymerase 1 and HOXD8 to regulate their mRNA stability [44, 45]. However, further investigation is required to ascertain whether NF90 and NF110 regulate the osteogenic differentiation of JBMMSCs by modulating the stability of osteogenic-related gene mRNAs. This enables the identification of potential target genes.

GO enrichment analysis of RNA-seq revealed that GO functions were associated with inflammatory, immune, and innate immune responses. Inflammasomes are innate immune receptors that play a pivotal role in inflammation [46]. The NLRP3 inflammasome is the most studied and comprises the protein NLRP3, apoptosis-associated speck-like protein, and pro-caspase-1 [47]. The increased incidence of BRONJ in mice resulting from Zol treatment correlates with NLRP3 inflammasome activation [48]. In addition, previous studies have shown that Zol induces apoptosis and reduces the osteogenic differentiation of murine osteoblast cell lines via the NLRP3/Caspase-1/gasdermin D pathway [9]. In addition, NLRP3 influences bone healing after tooth extraction. It has been demonstrated that NLRP3 inflammasome activation inhibits the osteogenic differentiation of JBMMSCs [49]. To investigate the relationship between NLRP3 inflammasome activation and BRONJ development, we measured the expression of NLRP3, Caspase-1 and IL-1 β in JBMMSCs following Zol stimulation. Our results showed that Zol increased the expression of NLRP3, Caspase-1, and IL-1 β in JBMMSCs. Subsequently, the expression of NLRP3 in

JBMMSCs overexpressing LINC01013, NF90, or NF110 was examined. We found that LINC01013 and NF90 reduced NLRP3 expression in Zol-treated JBMMSCs.

Conclusion

We elucidated the intricate molecular mechanisms underlying osteogenic differentiation during BP therapy, with particular focus on the involvement of HOXC8, LINC01013, and ILF3. Zol treatment increased HOXC8 expression, which suppressed LINC01013 levels in JBMMSCs and inhibited their osteogenic differentiation. The reduction in LINC01013 promoted NF90 and NF110 translocation from the nucleus to the cytoplasm, inhibiting the osteogenic differentiation of JBMMSCs. Meanwhile, the reduction in LINC01013 and cytoplasmic translocation of NF90 led to the increased expression of inflammation-related genes, which may contribute to the dysfunction of osteogenic differentiation in JBMMSCs. Our results indicate that LINC01013-ILF3 plays a significant regulatory role in osteogenic differentiation and inflammatory responses in JBMMSCs and serve as potential targets for the treatment of BRONJ. Future research should focus on further elucidating the molecular mechanisms underlying this pathway and exploring therapeutic interventions for BRONJ treatment.

Abbreviations

| | |
|--------------|---|
| ALP | Alkaline Phosphatase |
| ARS | Alizarin Red Staining |
| BP | Bisphosphonate |
| BRONJ | BP-Related Osteonecrosis of the Jaw |
| DIO2 | Iodothyronine Deiodinase 2 |
| FISH | Fluorescence in Situ Hybridization |
| GSDMC | Gasdermin C |
| HE | Hematoxylin and Eosin |
| HOXC8 | Homeobox C8 |
| IL-1 β | Interleukin-1 β |
| ILF3 | Interleukin Enhancer Binding Factor 3 |
| JBMMSCs | Jaw Bone Marrow Mesenchymal Stem Cells |
| lncRNAs | Long Non-Coding RNAs |
| MIAT | Myocardial Infarction-Associated Transcript |
| MGP | Matrix Gla Protein |
| MEDAG | Mesenteric Estrogen Dependent Adipogenesis |
| NLRP3 | NLR Family Pyrin Domain Containing 3 |
| RBPs | RNA-Binding Proteins |
| RT-qPCR | Real-Time Fluorescence quantitative Polymerase Chain Reaction |
| STAT3 | Signal Transducer and Activator of Transcription 3 |
| VIT | Vitrin |
| Zol | Zoledronic Acid |

Supplementary Information

The online version contains supplementary material available at <https://doi.org/10.1186/s13287-025-04467-3>.

Supplementary Material 1
Supplementary Material 2
Supplementary Material 3
Supplementary Material 4

Acknowledgements

We acknowledge the reviewers for their helpful comments. The authors declare that artificial intelligence is not used in this study. Schematic figure was created in BioRender.

Author contributions

JS performed the experiments, collected, and assembled data, analyzed and interpreted data, wrote the manuscript, and reviewed and edited the writing. WW and XF performed the methodology and software. HY participated in conceptualizing the project, obtaining funding, and reviewing and editing the writing. ZS conceptualized the project and reviewed and edited the writing. ZF conceptualized the project, acquired funding, and reviewed and edited the writing. All authors read and approved the final manuscript.

Funding

This work was supported by grants from the National Key Research and Development Program (2022YFA1104401 to Z.P.F.), National Natural Science Foundation of China (82201010 to H.Q.Y.), grants from Innovation Research Team Project of Beijing Stomatological Hospital, Capital Medical University (NO. CXTD202204 to Z.P.F.), Young Scientist Program of Beijing Stomatological Hospital, Capital Medical University (NO. YSP202415 to J.X.S.).

Data availability

Availability of data and materials' statement all additional files are included in the manuscript. The datasets used and analyzed in the current study are available from the corresponding author upon reasonable request.

Declarations

Ethics approval and consent to participate

The experiments involving human JBMMSCs in this study have been approved by the Ethical Committee of Beijing Stomatological Hospital, Capital Medical University (Title: The effect and mechanism of LINC01013 in preventing bisphosphonate-related osteonecrosis of the jaw; Approval number: CMUSH-IRB-KJ-PJ-2023-47; Date of approval: 2023-10-11). This study was adhered to the tenants of the Declaration of Helsinki. Human jaw bone were obtained with informed patient consent. The patients provided written informed consent for the use of the samples. The animal experiment was approved by the Animal Ethics Committee of the Beijing Stomatological Hospital of the Capital Medical University (Title: The effect and mechanism of LINC01013 in preventing bisphosphonate-related osteonecrosis of the jaw; Approval number: KQYY-202309-006; Date of approval: 2023-12-25).

Consent for publication

Not applicable.

Conflict of interest

The authors declared no competing interests.

Author details

¹Outpatient Department of Oral and Maxillofacial Surgery, School of Stomatology, Capital Medical University, Beijing, China
²Laboratory of Molecular Signaling and Stem Cells Therapy, Beijing Key Laboratory of Tooth Regeneration and Function Reconstruction, School of Stomatology, Capital Medical University, Beijing, China
³Beijing Laboratory of Oral Health, Capital Medical University, Beijing, China
⁴Research Unit of Tooth Development and Regeneration, Chinese Academy of Medical Sciences, Beijing, China

Received: 9 January 2025 / Accepted: 16 June 2025

Published online: 23 June 2025

References

- Lee ES, Tsai MC, Lee JX, Wong C, Cheng YN, Liu AC et al. Bisphosphonates and their connection to dental procedures: exploring Bisphosphonate-Related osteonecrosis of the jaws. *Cancers (Basel)*. 2023;15(22).

2. Kishimoto H, Noguchi K, Takaoka K. Novel insight into the management of bisphosphonate-related osteonecrosis of the jaw (BRONJ). *Jpn Dent Sci Rev.* 2019;55(1):95–102.
3. von Knoch F, Jaquiere C, Kowalsky M, Schaeren S, Alabre C, Martin I, et al. Effects of bisphosphonates on proliferation and osteoblast differentiation of human bone marrow stromal cells. *Biomaterials.* 2005;26(34):6941–9.
4. Patnirapong S, Singhatanadgit W, Chanruangvanit C, Lavanrattanakul K, Satravaha Y. Zoledronic acid suppresses mineralization through direct cytotoxicity and osteoblast differentiation inhibition. *J Oral Pathol Med.* 2012;41(9):713–20.
5. Hadad H, Matheus HR, Chen JE, Jounaidi Y, Souza F, Guastaldi FPS. Dose-dependent effects of Zoledronic acid on the osteogenic differentiation of human bone marrow stem cells (hBMSCs). *J Stomatol Oral Maxillofac Surg.* 2023;124(6):101479.
6. Fliefel R, El Ashwah A, Entekhabi S, Kumbrink J, Ehrenfeld M, Otto S. Bifunctional effect of Zoledronic acid (ZA) on human mesenchymal stem cells (hMSCs) based on the concentration level. *J Stomatol Oral Maxillofac Surg.* 2020;121(6):634–41.
7. Hu L, Wen Y, Xu J, Wu T, Zhang C, Wang J, et al. Pretreatment with bisphosphonate enhances osteogenesis of bone marrow mesenchymal stem cells. *Stem Cells Dev.* 2017;26(2):123–32.
8. Jin Y, Han X, Wang Y, Fan Z. METTL7A-mediated m6A modification of Corin reverses bisphosphonate-impaired osteogenic differentiation of orofacial BMSCs. *Int J Oral Sci.* 2024;16(1):42.
9. Duan Y, Li H, Dong X, Geng Z, Xu X, Liu Y. VEGF mitigates bisphosphonate-induced apoptosis and differentiation inhibition of MC3T3-E1 cells. *Exp Ther Med.* 2022;23(2):130.
10. Singhatanadgit W, Hankamolsiri W, Janvikul W. Geranylgeraniol prevents Zoledronic acid-mediated reduction of viable mesenchymal stem cells via induction of Rho-dependent YAP activation. *R Soc Open Sci.* 2021;8(6):202066.
11. Akintoye SO, Lam T, Shi S, Brahim J, Collins MT, Robey PG. Skeletal site-specific characterization of orofacial and iliac crest human bone marrow stromal cells in same individuals. *Bone.* 2006;38(6):758–68.
12. Stefanik D, Sarin J, Lam T, Levin L, Leboy PS, Akintoye SO. Disparate osteogenic response of mandible and iliac crest bone marrow stromal cells to pamidronate. *Oral Dis.* 2008;14(5):465–71.
13. Lee JT, Choi SY, Kim HL, Kim JY, Lee HJ, Kwon TG. Comparison of gene expression between mandibular and iliac bone-derived cells. *Clin Oral Investig.* 2015;19(6):1223–33.
14. Yang H, Liang Y, Cao Y, Cao Y, Fan Z. Homeobox C8 inhibited the osteo-/dentinogenic differentiation and migration ability of stem cells of the apical papilla via activating KDM1A. *J Cell Physiol.* 2020;235(11):8432–45.
15. Djebali S, Davis CA, Merkel A, Dobin A, Lassmann T, Mortazavi A, et al. Landscape of transcription in human cells. *Nature.* 2012;489(7414):101–8.
16. Hangauer MJ, Vaughn IW, McManus MT. Pervasive transcription of the human genome produces thousands of previously unidentified long intergenic noncoding RNAs. *PLoS Genet.* 2013;9(6):e1003569.
17. Dinger ME, Pang KC, Mercer TR, Mattick JS. Differentiating protein-coding and noncoding RNA: challenges and ambiguities. *PLoS Comput Biol.* 2008;4(11):e1000176.
18. Jiang S, Cheng SJ, Ren LC, Wang Q, Kang YJ, Ding Y, et al. An expanded landscape of human long noncoding RNA. *Nucleic Acids Res.* 2019;47(15):7842–56.
19. Jiang W, Chen Y, Sun M, Huang X, Zhang H, Fu Z, et al. LncRNA DGCR5-encoded polypeptide RIP aggravates SONFH by repressing nuclear localization of β -catenin in BMSCs. *Cell Rep.* 2023;42(8):112969.
20. Shao B, Zhou D, Wang J, Yang D, Gao J. A novel LncRNA SPIRE1/miR-181a-5p/PRLR axis in mandibular bone marrow-derived mesenchymal stem cells regulates the Th17/Treg immune balance through the JAK/STAT3 pathway in periodontitis. *Aging.* 2023;15(14):7124–45.
21. Yang H, Cao Y, Zhang J, Liang Y, Su X, Zhang C, et al. DLX5 and HOXC8 enhance the chondrogenic differentiation potential of stem cells from apical papilla via LINC01013. *Stem Cell Res Ther.* 2020;11(1):271.
22. Chung JH, Lu PH, Lin YH, Tsai MM, Lin YW, Yeh CT, et al. The long non-coding RNA LINC01013 enhances invasion of human anaplastic large-cell lymphoma. *Sci Rep.* 2017;7(1):295.
23. Wang W, Xu S, Di Y, Zhang Z, Li Q, Guo K, et al. Novel role of LINC01013/miR-6795-5p/FMN3L3 axis in the regulation of hepatocellular carcinoma stem cell features. *Acta Biochim Biophys Sin (Shanghai).* 2021;53(6):652–62.
24. Pham TP, Bink DI, Stanicek L, van Bergen A, van Leeuwen E, Tran Y, et al. Long Non-coding RNA Aeriec controls DNA damage repair via YBX1 to maintain endothelial cell function. *Front Cell Dev Biol.* 2020;8:619079.
25. Chignon A, Argaud D, Boulanger MC, Mkannez G, Bon-Baret V, Li Z, et al. Genome-wide chromatin contacts of super-enhancer-associated LncRNA identify LINC01013 as a regulator of fibrosis in the aortic valve. *PLoS Genet.* 2022;18(1):e1010010.
26. Ye J, Jin H, Pankov A, Song JS, Brelloch R. NF45 and NF90/NF110 coordinately regulate ESC pluripotency and differentiation. *RNA.* 2017;23(8):1270–84.
27. Castella S, Bernard R, Corno M, Fradin A, Larcher JC. ILF3 and NF90 functions in RNA biology. *Wiley Interdiscip Rev RNA.* 2015;6(2):243–56.
28. Liu Y, Wang H, Dou H, Tian B, Li L, Jin L, et al. Bone regeneration capacities of alveolar bone mesenchymal stem cells sheet in rabbit calvarial bone defect. *J Tissue Eng.* 2020;11:2041731420930379.
29. Wang L, Yang H, Lin X, Cao Y, Gao P, Zheng Y, et al. KDM1A regulated the osteo/dentinogenic differentiation process of the stem cells of the apical papilla via binding with PLOD2. *Cell Prolif.* 2018;51(4):e12459.
30. Choudhury NR, de Lima Alves F, de Andrés-Aguayo L, Graf T, Cáceres JF, Rappsilber J, et al. Tissue-specific control of brain-enriched miR-7 biogenesis. *Genes Dev.* 2013;27(1):24–38.
31. Yao RW, Wang Y, Chen LL. Cellular functions of long noncoding RNAs. *Nat Cell Biol.* 2019;21(5):542–51.
32. Cao Y, Wu J, Hu Y, Chai Y, Song J, Duan J, et al. Virus-induced lncRNA-BTX allows viral replication by regulating intracellular translocation of DHX9 and ILF3 to induce innate escape. *Cell Rep.* 2023;42(10):113262.
33. Nazitto R, Amon LM, Mast FD, Aitchison JD, Aderem A, Johnson JS, et al. ILF3 is a negative transcriptional regulator of innate immune responses and myeloid dendritic cell maturation. *J Immunol.* 2021;206(12):2949–65.
34. Song Y, Lin K, He S, Wang C, Zhang S, Li D, et al. Nano-biphasic calcium phosphate/polyvinyl alcohol composites with enhanced bioactivity for bone repair via low-temperature three-dimensional printing and loading with platelet-rich fibrin. *Int J Nanomed.* 2018;13:505–23.
35. Komori T. Functions of osteocalcin in bone, pancreas, testis, and muscle. *Int J Mol Sci.* 2020;21(20).
36. Maximiano WMA, da Silva EZM, Santana AC, de Oliveira PT, Jamur MC, Oliver C. Mast cell mediators inhibit osteoblastic differentiation and extracellular matrix mineralization. *J Histochem Cytochem.* 2017;65(12):723–41.
37. Chen X, Zhu X, Hu Y, Yuan W, Qiu X, Jiang T, et al. EDTA-Modified 17 β -Estradiol-Laden upconversion nanocomposite for Bone-Targeted hormone replacement therapy for osteoporosis. *Theranostics.* 2020;10(7):3281–92.
38. Huang H, Li L, Wen K. Interactions between long non-coding RNAs and RNA-binding proteins in cancer (Review). *Oncol Rep.* 2021;46(6).
39. Liu H, Hu L, Yu G, Yang H, Cao Y, Wang S, et al. LncRNA, PLXDC2-OT promoted the osteogenesis potentials of MSCs by inhibiting the deacetylation function of RBM6/SIRT7 complex and OSX specific isoform. *Stem Cells.* 2021;39(8):1049–66.
40. Khan MM, Khan MH, Kalim UU, Khan S, Junttila S, Paulin N, et al. Long intergenic noncoding RNA MIAT as a regulator of human Th17 cell differentiation. *Front Immunol.* 2022;13:856762.
41. Parrott AM, Walsh MR, Reichman TW, Mathews MB. RNA binding and phosphorylation determine the intracellular distribution of nuclear factors 90 and 110. *J Mol Biol.* 2005;348(2):281–93.
42. Xie F, Cui QK, Wang ZY, Liu B, Qiao W, Li N, et al. ILF3 is responsible for hyperlipidemia-induced arteriosclerotic calcification by mediating BMP2 and STAT1 transcription. *J Mol Cell Cardiol.* 2021;161:39–52.
43. Vrakas CN, Herman AB, Ray M, Kelemen SE, Scalia R, Autieri MV. RNA stability protein ILF3 mediates cytokine-induced angiogenesis. *Faseb J.* 2019;33(3):3304–16.
44. Song D, Huang H, Wang J, Zhao Y, Hu X, He F, et al. NF90 regulates PARP1 mRNA stability in hepatocellular carcinoma. *Biochem Biophys Res Commun.* 2017;488(1):211–7.
45. Zhuang Q, Ye B, Hui S, Du Y, Zhao RC, Li J, et al. Long noncoding RNA LncAIS downregulation in mesenchymal stem cells is implicated in the pathogenesis of adolescent idiopathic scoliosis. *Cell Death Differ.* 2019;26(9):1700–15.
46. Haneklaus M, O'Neill LA, Coll RC. Modulatory mechanisms controlling the NLRP3 inflammasome in inflammation: recent developments. *Curr Opin Immunol.* 2013;25(1):40–5.
47. Que X, Zheng S, Song Q, Pei H, Zhang P. Fantastic voyage: the journey of NLRP3 inflammasome activation. *Genes Dis.* 2024;11(2):819–29.
48. Zhang Q, Yu W, Lee S, Xu Q, Naji A, Le AD. Bisphosphonate induces osteonecrosis of the jaw in diabetic mice via NLRP3/Caspase-1-Dependent IL-1 β mechanism. *J Bone Min Res.* 2015;30(12):2300–12.

49. Geng Y, Bao C, Chen Y, Yan Z, Miao F, Wang T et al. NLRP3 deficiency improves bone healing of tooth extraction sockets through SMAD2/3-RUNX2 mediated osteoblast differentiation. *Stem Cells*. 2024.

Publisher's note

Springer Nature remains neutral with regard to jurisdictional claims in published maps and institutional affiliations.